Beyond Ventricular Fibrillation: Evaluating Tissue Strain in the Left and Right Atrium and their Role in *Commotio cordis* induced Atrial Fibrillation

Grant James Dickey[1], and Haojie Mao[1,2]
[1] Department of Biomedical Engineering, Western University, Canada
[2] Department of Mechanical & Materials Engineering, Western University, Canada.

ABSTRACT

Background: Impact induced cardiac arrhythmia, known as Commotio cordis, is primarily associated with ventricular fibrillation (VF). However, atrial fibrillation (AF) following chest impact in sports have been reported. Despite clinical significance, investigation regarding the mechanisms in which atrial stretch during repolarization can induce AF remain largely unexplored. This study aimed to bridge this gap by investigating chamber-specific susceptibility to arrhythmia using computational models that replicate real-world Commotio cordis impacts.

Methods: The Total Human Model for Safety (THUMS v7) was used to simulate Commotio cordis inducing impacts with baseball and lacrosse balls at 90 mph, targeting each of the four chambers of the heart. Peak maximum principal strain (MPS) values and distribution geometry from impacts were measured in each chamber and then mapped to a patient-specific electrophysiological (EP) heart model that was constructed using the PyAnsys-Heart platform. The mapped strain distributions from impacts were then used as electrical stimulus in the EP heart model, assessing the arrhythmogenic outcomes using volume ratio thresholds ranging from 1.0% to 8.0% in each chamber, to evaluate tissue volume requirements on arrhythmia susceptibility.

Results: The right atrium (RA) required the lowest volume ratio threshold (2.0%) to sustain a re-entrant arrhythmia, while the left atrium (LA) required the highest (8.0%). Additionally, arrhythmogenesis in all chambers was found to be influenced not only by the volume ratio threshold, but also the spatial distribution of tissue strain. Specifically, it was found that elongated strain geometry, rather than more localized geometries, were able to sustain re-entrant arrhythmia at lower volume ratio thresholds.

Conclusion: This study provides the first chamber-specific evidence that the RA is susceptible to AF from impact-induced tissue strain over the atrial chambers during atrial repolarization, suggesting its clinical significance in Commotio cordis. Additionally, the role of the RV was highlighted due to the peak MPS values experienced from impact, and the electrophysiological vulnerability to arrhythmia. These findings highlight the importance of incorporating atrial assessment in cardiac evaluation from chest impacts and provide a biomechanical foundation for future sports safety guidelines using real-world impact data.

This paper is a student paper from the 20th Injury Biomechanics Symposium and is published in a special issue of SAE International Journal of Transportation Safety.
It is preliminary work, has not been peer reviewed, and should not be cited because it is a work in progress.

INTRODUCTION

Disruption of cardiac rhythm from chest impacts, known as *Commotio cordis*, can result in dysrhythmias that vary in type, duration, and severity (Nesbitt et al., 2001) and are most often seen in sports. Historically, experimental research regarding *Commotio cordis* has been focused primarily on ventricular fibrillation (VF) (Link et al., 2001; Link et al., 1999; Maron et al., 2002; Maron et al., 1999). However, atrial fibrillation (AF) has also been documented following cases of *Commotio cordis* and has been hypothesized to be caused by atrial tissue stretch during atrial repolarization (Alkhamisi et al., 2021; Ota & Bratincsak, 2015). While VF results in total heart failure and requires immediate resuscitation (Grubic et al., 2022; Weisfeldt et al., 2010), AF is characterized by disorganized activity of the atria that impairs atrial contractility, and when untreated is associated with risks of ischemic stroke, heart failure, and death (Healey et al., 2012; Lubitz et al., 2013). Brief episodes of AF lasting as short as five minutes have been linked to a 67% increased risk of stroke (Go et al., 2018; Yang et al., 2022), emphasizing the clinical significance of this cardiac dysrhythmia.

Mechano-electro coupling (MEC) is the primary driver for arrhythmogenesis in *Commotio cordis*, as it involves the relationship between cardiac tissue stretch and the induction of electrical excitation (Quinn & Kohl, 2021). During the cardiac repolarization phase, tissue becomes electrically heterogeneous, and particularly vulnerable. In the case of *Commotio cordis*, external impacts to the chest results in a stretch of the cardiac tissue, causing a premature depolarization stimulus which may evolve into a sustained re-entrant wavefront (Quinn et al., 2017; Wijesurendra & Casadei, 2019). While this mechanism is well-established in the ventricles, it is not fully understood in the atrial chambers. An additional consideration is whether mechanical stretch of the atrial tissue can generate sufficient excitation to sustain re-entry in the atrial chambers. This depends on the source-to-sink balance which considers the relationship between the excited (depolarized) tissue 'source' and the surrounding tissue 'sink'. For sustained re-entry to occur, the size of the 'source' must overcome the surrounding 'sink'. While computational (Xie et al., 2010) and optogenetic studies (Zaglia et al., 2015) have investigated source-to-sink requirements in the ventricles, investigations into the atrial chamber requirements are lacking.

To investigate these gaps in the literature, we have utilized a full-body computational model to replicate real-world chest impacts using two projectiles most associated with *Commotio cordis*, baseballs and lacrosse balls (Maron et al., 2011; Shore et al., 2024). A patient specific electrophysiological heart model was utilized to assess arrhythmic response to stimulus. These projectiles were modeled to impact all four cardiac chambers under standardized conditions using a whole human body model, allowing for the analysis of localized tissue strain in each chamber. The resulting peak tissue strain was then mapped to the patient-specific electrophysiological heart model where electrical stimulus patterns of varying volume ratio thresholds were used to determine the relationship between stimulus volume and arrhythmia induction. The aim of this study was to address a fundamental gap in *Commotio cordis* research, by providing the first chamber-specific analysis that compares the arrhythmic potential of the atrial and ventricular chambers using real-world impact data. By characterizing both mechanical and electrophysiological vulnerability, this study systematically evaluated whether the observed volume ratio thresholds and spatial strain distributions were sufficient to trigger sustained re-entrant arrythmia.

This paper is a student paper from the 20th Injury Biomechanics Symposium and is published in a special issue of SAE International Journal of Transportation Safety.
It is preliminary work, has not been peer reviewed, and should not be cited because it is a work in progress.

METHODS

Impact Simulations of Human Body Model

The Total Human Model for Safety (THUMS) v7 computational model developed by TOYOTA was used to simulate *Commotio cordis* impacts in a human body model representing an adult male 50^{th} percentile (height: 173 cm, weight: 77.3 kg) (Figure 1A). Projectile impacts were modeled using both baseball and lacrosse balls simulated at 90 mph (40 m/s). Chamber-specific impact locations were selected to isolate the mechanical response in all four heart chambers, maximizing local tissue strain and allowing for a comparative analysis across cardiac regions under identical loading conditions. The baseball and lacrosse ball computational models were constructed using standard dimensions and material properties of official baseball and lacrosse balls (Figure 1B). The impact velocity of 90 mph was chosen to replicate velocities observed in documented cases of *Commotio cordis* in adults, particularly in baseball and lacrosse (Maron et al., 2011; Shore et al., 2024). Real-world cases of AF from *Commotio cordis* in the literature (Alkhamisi et al., 2021; Ota & Bratincsak, 2015) were not detailed enough to accurately replicate. However, these scenarios provided an evidence-based foundation for simulating impacts to assess whether atrial stretch from atrial impacts would induce AF in the atrial chambers. Peak maximum principal strain (MPS) was used as a proxy indicator for measuring cellular deformation at the level of cardiomyocytes (Dickey et al., 2023; Dickey et al., 2021; Dickey et al., 2022).

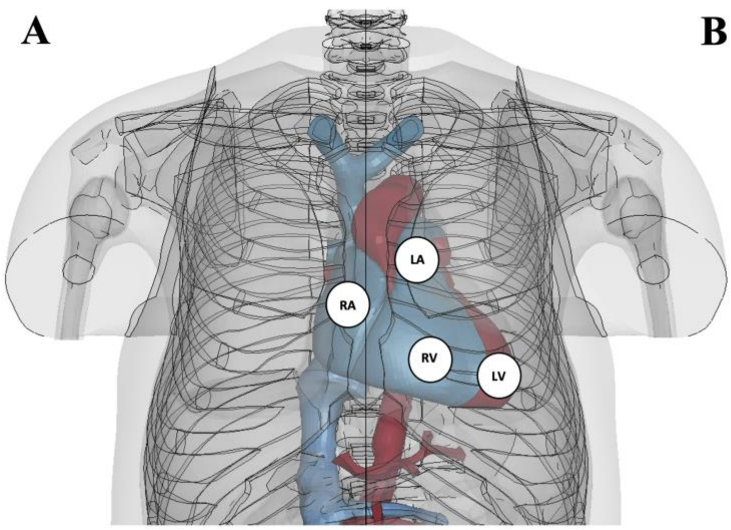

B

	Lacrosse Ball	Baseball
Velocity	90 mph (40 m/s)	90 mph (40 m/s)
Mass	142 g (0.042 kg)	142 g (0.042 kg)
Diameter	64.7 mm (0.0647 m)	73.5 mm (0.0735 m)

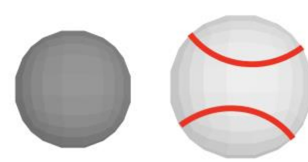

Figure 1. A) Impact locations over each chamber of the heart, right atrium (RA), left atrium (LA), right ventricle (RV), left ventricle (LV) of the THUMS v7 human body model. B) Mass, velocity and diameter for the lacrosse ball and baseball projectiles, projectiles are not to scale.

Construction of Electrophysiological Heart Model

The PyAnsys-Heart platform was integrated into this study to build a computational electrophysiological (EP) heart model based on patient specific CT scans (Rodero et al., 2021; Strocchi et al., 2020) (Figure 2A). Electrical propagation within the heart was simulated using a monodomain model which assumes an equal anisotropy ratio between the intracellular conductivity tensor and the extracellular conductivity tensor (Hoeijmakers, 2023), while also maintaining accuracy (Potse et al., 2006). Electrical stimulus was derived using the ten Tusscher ionic model which incorporates experimental data from major ion channels from human myocytes (ten Tusscher et al., 2004). The cardiac tissue was modelled using a hyperelastic orthotropic material with a non-linear stress-strain relationship (Holzapfel & Ogden, 2009). To ensure accurate impulse propagation, the SA and AV nodes, Purkinje network and bundle branches were included in the model (Hoeijmakers, 2023) (Figure 2B), while fiber orientation and spatial arrangement for ventricular myocytes were considered using a rule-based algorithm (Bayer et al., 2012). The heart geometry was discretized using a tetrahedral mesh with an average element edge length of 1.6mm. Each chamber in the heart varied in the total amount of elements, 18,048 in the left atrium (LA), 19,399 in the right atrium (RA), 64,995 in the left ventricle (LV), and 38,194 in the right ventricle (RV).

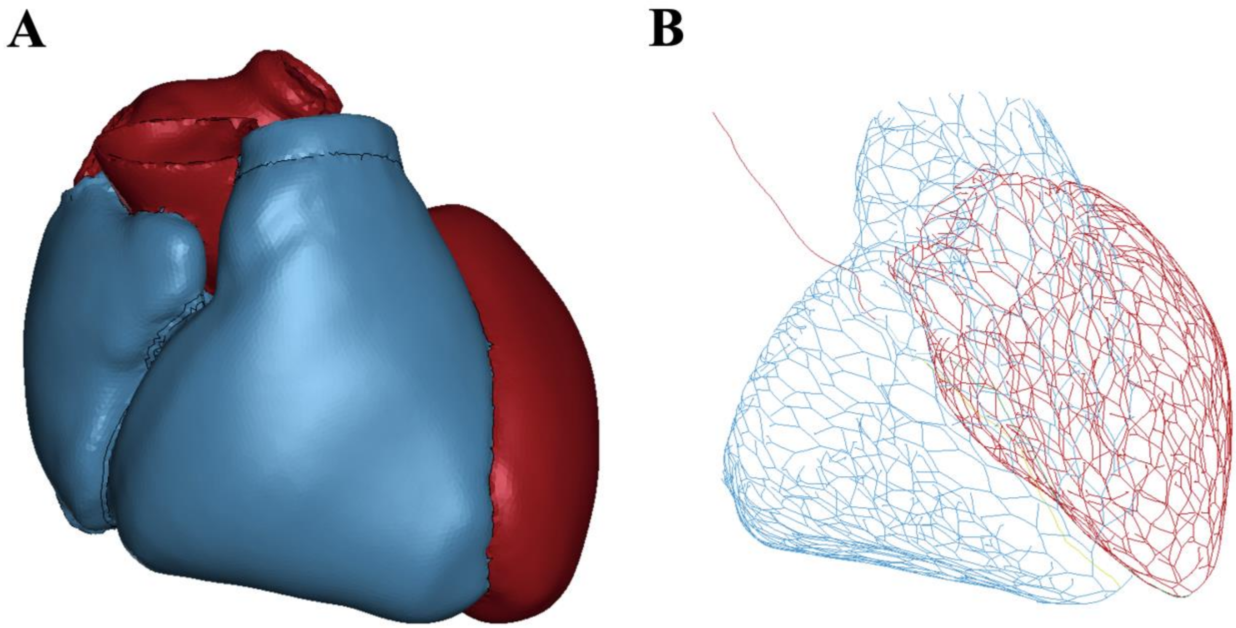

Figure 2. A) Frontal view of EP-heart model including the RA and RV (blue), LA and LV (red). B) Interior electrical network responsible for electrical activation including the SA and AV nodes, right and left Purkinje network and bundle branches.

Mapping of Mechanical Strain to Electrophysiological Model

To simulate MEC in the EP-heart model, peak MPS data from the THUMS v7 impacts were used to define the location and geometry of electrical stimuli. Peak MPS values from each projectile impact scenario were extracted across the surface of the heart, and for each chamber and impact condition the six elements exhibiting the highest MPS were identified and their values averaged to represent peak local deformation. A measurement-based nodal correspondence technique was used on the THUMS v7 heart model. Specifically, the elements exhibiting peak MPS values from impact were spatially measured and transferred to the EP-heart model using distance-based matching relative to anatomical landmarks in millimeters (mm). This ensured that

This paper is a student paper from the 20th Injury Biomechanics Symposium and is published in a special issue of SAE International Journal of Transportation Safety.
It is preliminary work, has not been peer reviewed, and should not be cited because it is a work in progress.

the mechanical deformation that was observed in the THUMS v7 simulations was accurately projected in each chamber of the EP-heart model.

Simulation Protocol and Data Analysis

The physics software to solve the simulations used in this study for both THUMS v7 and the EP-Heart model was LS-DYNA R16 MPP double-precision with MS-MPI, while pre- and postprocessing was prepared and analyzed with LS-PrePost v4.12.0. A total of 8 chest impact simulations were conducted using the THUMS v7 model, 4 with the baseball and 4 with the lacrosse ball. Each simulation targeted one of the 4 cardiac chambers, resulting in chamber-specific mechanical loading conditions. In each simulation, peak MPS was extracted from all 4 cardiac chambers, producing 32 chamber-specific tissue values. The 6 highest element MPS values were averaged out to remove potential outliers, and this averaged value was reported (Table 1).

For each impact simulation, the time point used for MPS data collection was standardized to be the time when the targeted chamber reached peak MPS. The remaining three chambers were assessed at this time as well, ensuring consistency across all impact conditions. In the EP-heart model, 72 simulations were conducted across both baseball and lacrosse ball projectiles. To isolate the electrophysiological effect of direct mechanical impacts, only the chamber that was the direction of impact was simulated in the EP-heart model. A depolarization stimulation amplitude of +50 mV was applied over the trailing edge of the repolarization wave during atrial repolarization in the atrial chambers and during ventricular repolarization in the ventricular chambers, a method consistent for inducing arrhythmia (Quinn et al., 2017). Simulations were performed using stimulus volume ratio thresholds ranging from 1.0% to 8.0% of each chamber's surface area, with an additional threshold of <1.0% which corresponded to each specific chamber's peak MPS value. Each stimulus volume ratio was matched with its corresponding MPS value to assess the mechanical stretch values seen at these volume ratio thresholds which were able to trigger ectopic electrical activity. Arrhythmia was defined as a sustained, self-propagating re-entrant circuit persisting of a minimum of two cardiac cycles following stimulus initiation. The outcomes were classified based on the presence of re-entry under each volume ratio threshold.

RESULTS

Chamber-Specific Tissue Strain in Human Body Model (THUMS v7)

Simulations using the THUMS v7 model with the baseball and lacrosse ball impacts demonstrated distinct differences in peak MPS. Across all four chambers, the RV consistently experienced the highest or second-highest peak MPS values. The highest values observed were in the RV from the baseball (0.436) and lacrosse ball (0.453) during RV-directed impacts (Table 1). Both ventricular chambers generally exhibited higher peak MPS when compared to the atrial chambers which is largely due to their anterior exposure to impact from the rib cage and sternum and overall larger surface area (Figure 2A).

*This paper is a student paper from the 20th Injury Biomechanics Symposium and is published in a special issue of SAE International Journal of Transportation Safety.
It is preliminary work, has not been peer reviewed, and should not be cited because it is a work in progress.*

Table 1. Cardiac Tissue peak MPS values across all chambers (LA, RA, LV, RV) of the heart in both baseball and lacrosse 90 mph impacts, and impact locations (LA, RA, LV, RV).

		Baseball Impact 90 mph	Lacrosse Impact 90 mph
Impact Location	**Heart Chamber**	**Peak MPS**	**Peak MPS**
LA	LA	0.138	0.144
	RA	0.245	0.257
	LV	0.130	0.134
	RV	0.360	0.375
RA	LA	0.017	0.021
	RA	0.350	0.383
	LV	0.015	0.015
	RV	0.147	0.167
LV	LA	0.050	0.059
	RA	0.110	0.158
	LV	0.306	0.344
	RV	0.362	0.384
RV	LA	0.066	0.051
	RA	0.162	0.181
	LV	0.177	0.178
	RV	0.436	0.453

The RA, which lies adjacent to the RV and sits anteriorly beneath the sternum, also exhibited substantial peak MPS during the RA-directed impact condition, with values of 0.350 (baseball) and 0.383 (lacrosse), which was second only to the RV peak MPS values. During the LA and RA-directed impacts in both baseball and lacrosse, the RA peak MPS surpassed the LV, highlighting the exposure of the RA's anatomical positioning during chest impacts. In contrast, the LA consistently exhibited the lowest peak MPS values. In the non-targeted impacts, the LA peak MPS ranged from 0.017 in the RA-directed baseball impacts to 0.066 in the RV-directed impacts. When the impact was LA-directed, however, the LA reached a peak of 0.138 and 0.144 peak MPS in both projectile impacts. These results illustrate how the posterior positioning of the LA shields this chamber behind the other 3 chambers, as it is less exposed to anterior chest impacts.

The lacrosse ball impacts, which had a smaller surface area, generated slightly higher peak MPS values than the baseball impacts across all chambers in the LA, RA, and LV impact locations, despite having identical initial kinetic energy. Among these impact locations, the lacrosse ball impacts had an increased peak MPS ranging from 0.004 (LV) to 0.015 (RV) across all chambers in the LA-directed impacts, while ranging from 0.000 (LV) to 0.033 (RA) in the RA-directed impacts when compared to baseball cases. In the RV-directed impacts the peak MPS values were nearly identical in the LV chamber, however, they were 0.015 (LA) to 0.020 (RA) higher in the atrial chambers from baseball impacts compared to lacrosse impacts. These were the only cases where the baseball impacts exceeded lacrosse.

Volume Ratio Thresholds and Arrhythmic Outcomes in EP-Heart Model

Simulations using the EP-heart model revealed chamber-specific sensitivity to arrhythmia induction across varying volume ratio thresholds. Each volume ratio threshold was paired with the corresponding MPS value derived from the THUMS v7 impacts (Table 2 & Table 3), while the volume ratio thresholds were tested to determine the minimum requirement necessary to sustain re-entry in each chamber. The strain geometry created by impacts from the THUMS v7 model that were mapped to the EP-heart model resulted in differences in the sustainability of arrhythmic outcome at identical volume ratio thresholds in the same chamber.

Table 2. Volume ratio thresholds for the EP-heart model and their corresponding peak MPS for inducing sustained re-entry (red) or no arrhythmic outcome (green) in baseball 90 mph impacts.

Baseball 90 mph Impact Reconstruction								
	LA impact LA chamber		**RA impact RA chamber**		**LV impact LV chamber**		**RV impact RV chamber**	
Volume Ratio Threshold (%)	MPS	Arrhythmic Outcome	MPS	Arrhythmic Outcome	MPS	Arrhythmic Outcome	MPS	Arrhythmic Outcome
8.0	0.085	***Re-entry***	0.210	***Re-entry***	0.215	***Re-entry***	0.360	***Re-entry***
7.0	0.090	-	0.215	***Re-entry***	0.220	***Re-entry***	0.365	***Re-entry***
6.0	0.100	-	0.220	***Re-entry***	0.230	***Re-entry***	0.370	***Re-entry***
5.0	0.105	-	0.230	***Re-entry***	0.240	***Re-entry***	0.380	***Re-entry***
4.0	0.110	-	0.250	***Re-entry***	0.250	-	0.390	***Re-entry***
3.0	0.115	-	0.270	***Re-entry***	0.260	-	0.400	-
2.0	0.125	-	0.300	***Re-entry***	0.280	-	0.410	-
1.0	0.130	-	0.320	-	0.300	-	0.420	-
<1.0	0.138	-	0.383	-	0.344	-	0.436	-

Table 3. Volume ratio thresholds for the EP-heart model and their corresponding peak MPS for inducing sustained re-entry (red) or no arrhythmic outcome (green) in lacrosse 90 mph impacts.

Lacrosse 90 mph Impact Reconstruction								
	LA impact LA chamber		**RA impact RA chamber**		**LV impact LV chamber**		**RV impact RV chamber**	
Volume Ratio Threshold (%)	MPS	Arrhythmic Outcome	MPS	Arrhythmic Outcome	MPS	Arrhythmic Outcome	MPS	Arrhythmic Outcome
8.0	0.085	***Re-entry***	0.220	***Re-entry***	0.250	***Re-entry***	0.330	***Re-entry***
7.0	0.090	-	0.230	***Re-entry***	0.255	***Re-entry***	0.340	***Re-entry***
6.0	0.100	-	0.250	***Re-entry***	0.260	***Re-entry***	0.350	***Re-entry***
5.0	0.105	-	0.270	***Re-entry***	0.270	-	0.360	***Re-entry***
4.0	0.110	-	0.290	***Re-entry***	0.280	-	0.380	***Re-entry***
3.0	0.115	-	0.300	***Re-entry***	0.290	-	0.400	***Re-entry***
2.0	0.125	-	0.320	***Re-entry***	0.295	-	0.410	-
1.0	0.135	-	0.340	-	0.300	-	0.430	-
<1.0	0.144	-	0.350	-	0.306	-	0.453	-

This paper is a student paper from the 20th Injury Biomechanics Symposium and is published in a special issue of SAE International Journal of Transportation Safety.
It is preliminary work, has not been peer reviewed, and should not be cited because it is a work in progress.

Among all chambers the RA consistently had lower volume ratio threshold requirements to sustain re-entry. Moreover, the two atrial chambers responded differently to stimulus thresholds. While the RA was highly sensitive, sustaining re-entrant arrhythmia with a volume ratio threshold as low as 2.0%, the LA remained non-arrhythmogenic until reaching the maximum testing threshold of 8.0%. These results were consistent across both baseball and lacrosse impacts, identifying a gap between arrhythmic vulnerability between the atrial chambers based on these specific stimulus conditions.

In the ventricular chambers, the gap in volume ratio threshold sensitivity between each chamber was less than what was seen in the atrial chambers, but still notable. During baseball impacts, the RV sustained re-entry with a volume ratio of 4.0%, slightly lower than the 5.0% required in the LV. However, in the lacrosse ball simulations the gap widened as the RV triggered sustained re-entry at 3.0%, while the LV required a higher threshold of 6.0%. The chamber-specific volume ratio thresholds and their corresponding MPS for inducing sustained re-entry (red) are visualized in Figure 3.

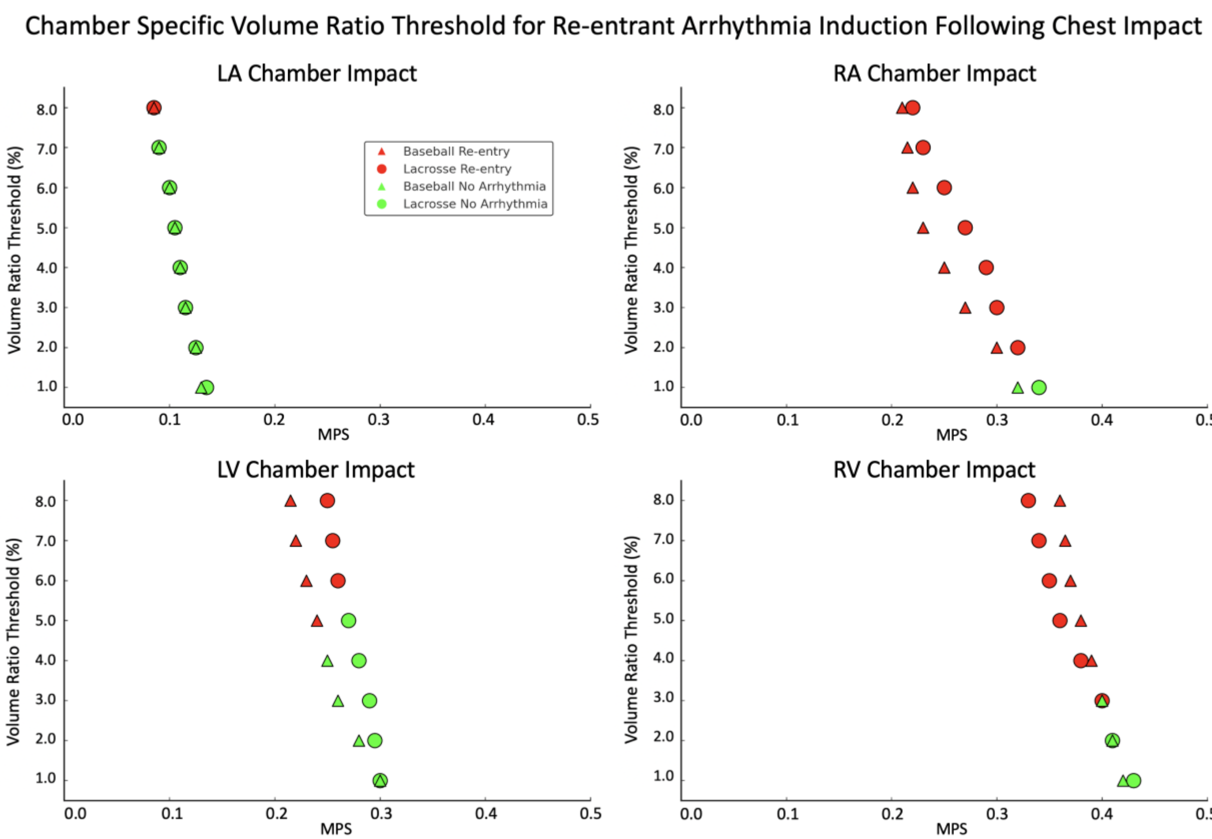

Figure 3. Volume ratio threshold required to induce re-entry are shown across atrial and ventricular chambers for baseball (triangles) and lacrosse (circles) impacts and their corresponding MPS values. Stimulus volume ratio thresholds from 1.0% to 8.0% of each chamber were simulated, red data points indicate when re-entry occurred, while green indicates no arrhythmic response from stimulus.

This paper is a student paper from the 20th Injury Biomechanics Symposium and is published in a special issue of SAE International Journal of Transportation Safety.
It is preliminary work, has not been peer reviewed, and should not be cited because it is a work in progress.

While comparing the arrhythmic outcomes between the baseball and lacrosse impacts, the lacrosse was able to sustain a re-entrant arrhythmia at 1.0% volume ratio threshold lower than the baseball impacts in the LV (5.0% vs. 6.0%) and the RV (3.0% vs. 4.0%). Notably, in the RV with identical volume ratio thresholds (3.0%), but different stimulus shapes the baseball (Figure 4A) created a more localized rectangular stimulus pattern when compared to the lacrosse ball (Figure 4B), which had a more elongated pattern which allowed it to spread down to the apex of the ventricles and sustain a re-entrant arrhythmia.

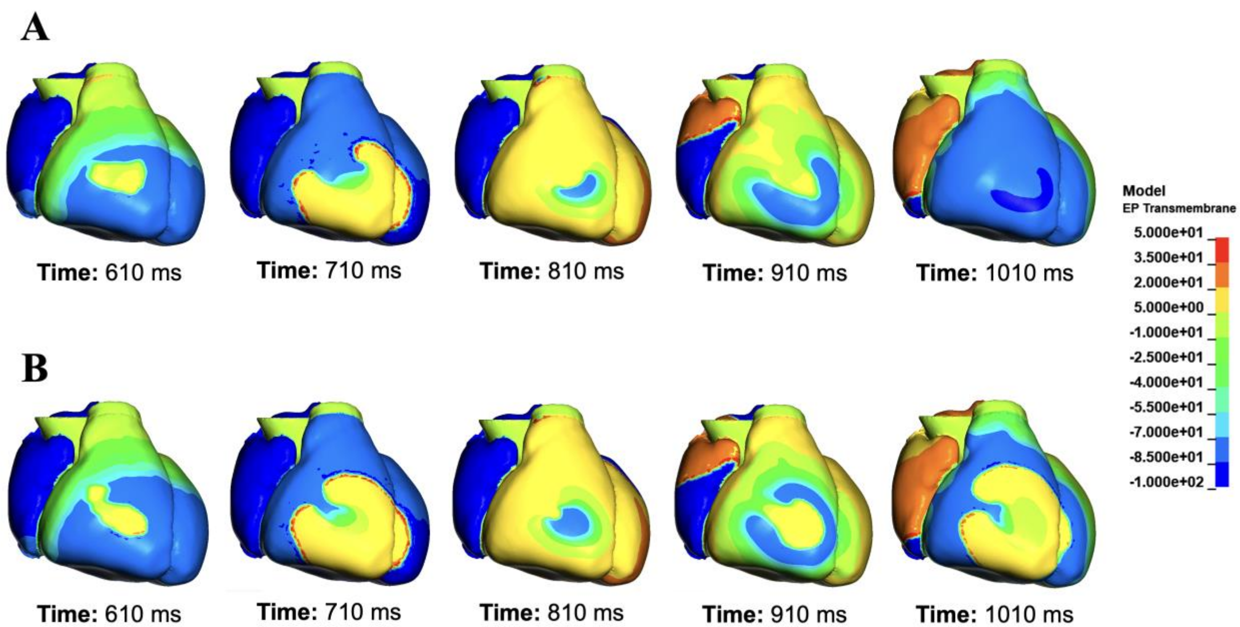

Figure 4. Time history from point of stimulus at 610 ms to 1010 ms of strain distribution patterns at identical volume ratio threshold (3.0%) between baseball and lacrosse impacts over the RV. (A) The baseball impact was unable to sustain re-entry and fizzled out by 1010 ms. (B) The lacrosse stimulus shape stretched down to the apex of the ventricles which influenced the ability to sustain re-entry.

DISCUSSION

Chamber-Specific Arrhythmogenic Susceptibility

This study provides the first computational evidence that atrial tissue, specifically the RA, is vulnerable to stretch-induced re-entrant arrhythmia during baseball and lacrosse ball impacts to the chest. The RA consistently exhibited lower volume ratio threshold requirements for sustaining a re-entrant arrhythmia when compared to the LA and even demonstrated lower requirements when compared to both ventricular chambers (Figure 3). Our findings show that the RA was four times more sensitive to sustained re-entry than the LA in both baseball and lacrosse impacts, suggesting the LA is considerably less arrhythmogenic at this specific stimulus location. Furthermore, while the lacrosse ball impacts generated consistently higher peak MPS values than the baseball across most impact scenarios, our data suggests that the arrhythmogenic potential depended not only on

This paper is a student paper from the 20th Injury Biomechanics Symposium and is published in a special issue of SAE International Journal of Transportation Safety.
It is preliminary work, has not been peer reviewed, and should not be cited because it is a work in progress.

the volume ratio threshold, but also on the spatial orientation of these strain-induced stimuli. This was evident when translating the peak MPS geometry in the THUMS v7 model to the EP-heart model, as this resulted in slightly more arrhythmogenic outcomes depending on the geometric distribution at the same volume ratio threshold. In the ventricular impacts, geometric differences in strain patterns at identical volume ratio thresholds influenced whether re-entry was sustained. This suggests that arrhythmia vulnerability is not only determined by the amount of tissue excited, but also how that excitation is distributed anatomically in each chamber.

Atrial Involvement in *Commotio cordis*: Bridging the Gap

Our findings have bridged a critical gap in *Commotio cordis* research by demonstrating how atrial tissue can induce sustained re-entrant arrhythmia following deformation from real-world chest impacts, particularly in the context of atrial tissue stretch during atrial repolarization. Anatomically, this vulnerability can be explained by the positioning of the RA posterior to the sternum, making it particularly susceptible to directly absorb forces from chest impacts. In contrast, the LA at most angles, is shielded by the RA, RV, LV, pulmonary artery and aortic arch. This resulted in the LA having the lowest peak MPS values across most impact scenarios, even during LA-directed impacts the RV and RA experienced higher peak MPS values. Based on anatomical positioning, peak MPS values across all impact directions (Table 1) and the electrophysiological response from each atrial chamber (Table 2 & Table 3), the RA is at a unique predisposition to develop AF from *Commotio cordis* inducing impacts, while the LA is not.

Source-to-Sink Requirements in the EP-Heart Model

Quantifying the requirements between the volume of excited cardiac tissue and arrhythmogenesis is an ongoing discussion (source-to-sink). The successful propagation of an extra stimulus due to stretch requires the excited 'source' to overcome the resting 'sink' (Xie et al., 2010). Volume ratio thresholds served as a measure of the minimum 'source' required to overcome the electrotonic 'sink' for sustaining a re-entrant arrhythmia. Our simulations revealed chamber specific differences in the minimum source required to sustain re-entry, with the RA requiring the lowest threshold, and the LA requiring the highest. While it is not immediately clear why this gap in source requirements exists between the atrial chambers, one possible explanation is that the location of the stimulus influences the electrophysiological effect. Specifically, the stimuli occurring on the superficial surface of the RA (Figure 5A) may propagate more effectively than the stimuli that originated deep within the myocardial wall in the LA (Figure 5B) which may have been surrounded by a larger 'sink' as it was connected with the walls of the RA and LV. A systematic investigation into how the stimulus depth, orientation and location with respect to chamber anatomy may provide more insight into these arrhythmic outcomes.

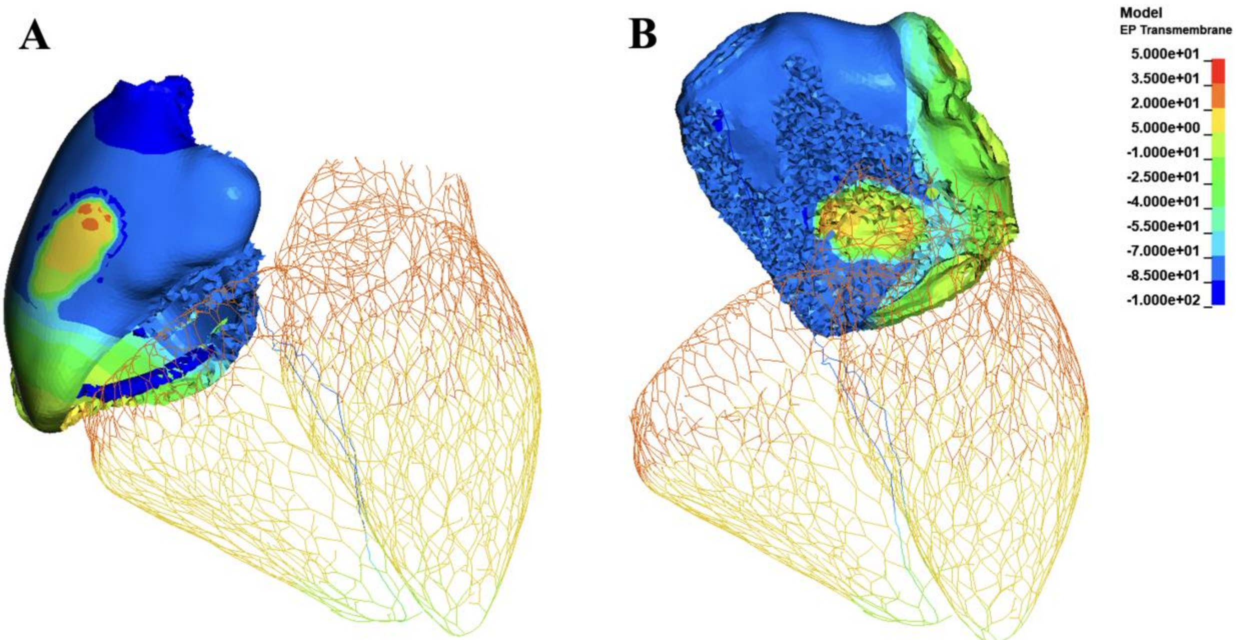

Figure 5. Frontal view of the origin for each electrical stimulus in the EP-heart model at volume ratio threshold 2.0%, based on peak MPS location and shape from THUMS v7 model. Purkinje fibers and bundle branches included for context of anatomical positioning. A) RA with electrical stimulus originating on superficial surface of the chamber, B) EP-heart model LA with electrical stimulus originating on the inside of the heart, with tissue connecting to the LV.

A New Mechanism in Arrhythmic Vulnerability

It is understood that arrhythmic vulnerability in *Commotio cordis* is primarily governed by MEC (Kohl et al., 2001; Quinn & Kohl, 2021) and source-to-sink requirements, however, our results have illustrated that the spatial geometry of mechanical strain can critically influence whether a re-entrant arrhythmia will be sustained or not. The elongated strain patterns (Figure 4B) were more effective in moving the excited source along the conduction pathways which allowed it to drag and spread more efficiently. In contrast, the rectangular stimulus that was observed in the baseball impact (Figure 4A) created a more localized source, failing to sustain propagation despite having the same volume ratio threshold. These findings reinforce us to not only consider the volume ratio threshold, but also the spatial geometry of the mechanical stimulus, as these may prove to be critically involved in the vulnerability of an arrhythmia from *Commotio cordis*.

Clinical Implications of the RA and the Role of the RV

The identification of the RA as a highly susceptible chamber to stretch-induced arrhythmia from chest impacts has broadened our understanding of *Commotio cordis* beyond the conventionally reported on VF. These simulations have provided evidence that adds AF to the arrhythmic spectrum from *Commotio cordis* as a significant outcome in baseball and lacrosse. Clinically, our findings indicate that cardiac monitoring after chest impacts should include early detection of AF, as this could improve timely interventions to reduce complications in athletes. While AF can be asymptomatic and is not immediately lethal, it is also the most commonly sustained arrhythmia (Chugh et al., 2014), and early detection of *Commotio cordis* induced AF could greatly reduce the risk of ischemic stroke (Yang et al., 2022).

Our results have also highlighted an important role of the RV in mechanical and arrhythmogenic vulnerability. The RV experienced the highest peak MPS across almost all impact scenarios, only coming second to the RA during RA-directed impacts. Similar to the vulnerability of the RA, the RV is particularly vulnerable during chest impacts due to the anterior positioning of the chamber, and specifically, under most impact angles and locations the RV acts as a shield, particularly to the LA. The importance of this contribution to the literature regarding our findings of the RV can be attributed to the lack of focus on the RV during *Commotio cordis* research, as swine models have stated that the LV is the chamber responsible for inducing *Commotio cordis* (Link, 2012; Link et al., 2001). In contrast, focus on the role of the RV in MEC during lamb studies has shown that stretch of the RV can trigger arrhythmogenesis (Greve et al., 2001), and stretch causing dispersion of repolarization in the RV was linked to premature ventricular beats, strengthening the argument that the RV plays a role in MEC in *Commotio cordis* (Chen et al., 2004).

Limitations and Future Directions

This study has a couple limitations that we acknowledge. The strain mapping between the THUMS v7 and EP-heart model used manual nodal-correspondence which, while ensuring anatomical accuracy, is limited by the slightly different heart geometries between the THUMS v7 heart and the EP-heart model. Our future work will improve accuracy by developing patient-specific heart models based on clinical CT scans. Furthermore, the EP-heart model assumed that all applied stimuli were equal (+50 mV), and did not adjust stimuli strength depending on peak MPS values across impact scenarios. This assumption was made due to the lack of evidence in the literature regarding strain thresholds within cardiac tissue that are required to initiate an action potential, and we therefore assumed that all peak MPS values would elicit an ectopic beat. While research regarding strain thresholds are ongoing, an optical mapping study using rabbit tissue has suggested strain thresholds within medium ranges (0.10 to 0.15) may be more arrhythmogenic than low (<0.10) or excessively high strains (>0.20) (Seo et al., 2010). Additionally, these simulations were conducted with a static heart which does not account for the mechanical changes between diastole and systole and therefore may influence strain distribution and/or electrical propagation. However, as *Commotio cordis* has been shown to be triggered in as little as 10-20 ms, it is possible than these changes would have little to no effect on the beating myocardium. Future studies plan to integrate the beat-to-beat dynamics of the cardiac cycle into the EP-heart model to determine the influence this may have.

CONCLUSIONS

This study has provided the first chamber-specific computational analysis that suggests the RA is both mechanically and electrophysiologically susceptible to stretch-induced arrhythmia from *Commotio cordis*, establishing AF as an arrhythmic outcome. Using real-world impacts seen in baseball and lacrosse, we successfully demonstrated that arrhythmic vulnerability is not only dependent on the volume of excited tissue, but also the spatial geometry of the tissue strain distribution. Additional findings illustrated that the RV is particularly vulnerable due to the anatomical position of the chamber, even more than the LV during these specific impact conditions. Clinically, these findings highlight the importance of early atrial monitoring following chest trauma, particularly given the significant stroke risk associated with even transient episodes of AF. The insights from this study have expanded our understanding of the arrhythmic spectrum seen in *Commotio cordis* and laid the foundation for future work for comprehensively characterizing a full four-chamber analysis beyond the conventionally analyzed LV.

ACKNOWLEDGEMENTS

We acknowledge the support of NSERC and Canada Research Chairs. We acknowledge Martijn Hoeijmakers, Karim El Houari, Pierre L'Eplattenier, and Wenfeng Ye from ANSYS Inc. for the support with access to the PyAnsys-Heart platform and EP-heart model.

REFERENCES

Alkhamisi, A., Carek, S. M., Dillon, M. C., & Clugston, J. R. (2021). Atrial Fibrillation Induced From Commotio Cordis. *Clin J Sport Med*, *31*(4), e213-e215. https://doi.org/10.1097/JSM.0000000000000787

Bayer, J. D., Blake, R. C., Plank, G., & Trayanova, N. A. (2012). A novel rule-based algorithm for assigning myocardial fiber orientation to computational heart models. *Ann Biomed Eng*, *40*(10), 2243-2254. https://doi.org/10.1007/s10439-012-0593-5

Chen, R. L., Penny, D. J., Greve, G., & Lab, M. J. (2004). Stretch-induced regional mechanoelectric dispersion and arrhythmia in the right ventricle of anesthetized lambs. *Am J Physiol Heart Circ Physiol*, *286*(3), H1008-1014. https://doi.org/10.1152/ajpheart.00724.2003

Chugh, S. S., Havmoeller, R., Narayanan, K., Singh, D., Rienstra, M., Benjamin, E. J.,…Murray, C. J. (2014). Worldwide epidemiology of atrial fibrillation: a Global Burden of Disease 2010 Study. *Circulation*, *129*(8), 837-847. https://doi.org/10.1161/CIRCULATIONAHA.113.005119

Dickey, G. J., Bian, K., Islam, S. U., Khan, H. R., Rohr, S., & Mao, H. (2023). Advancing Commotio cordis Safety Standards Using the Total Human Models for Safety (THUMS). *Ann Biomed Eng*, *51*(9), 2070-2085. https://doi.org/10.1007/s10439-023-03235-9

Dickey, G. J., Bian, K., Khan, H. R., & Mao, H. (2021). Developing commotio cordis injury metrics for baseball safety: unravelling the connection between chest force and rib deformation to left ventricle strain and pressure. *Comput Methods Biomech Biomed Engin*, 1-10. https://doi.org/10.1080/10255842.2021.1948022

Dickey, G. J., Bian, K., Liu, X., Khan, H. R., & Mao, H. (2022). Identifying Vulnerable Impact Locations to Reduce the Occurrence of Deadly Commotio Cordis Events in Children's Baseball: A Computational Approach. *J Biomech Eng*, *144*(5). https://doi.org/10.1115/1.4052886

Go, A. S., Reynolds, K., Yang, J., Gupta, N., Lenane, J., Sung, S. H.,…Solomon, M. D. (2018). Association of Burden of Atrial Fibrillation With Risk of Ischemic Stroke in Adults With Paroxysmal Atrial Fibrillation: The KP-RHYTHM Study. *JAMA Cardiol*, *3*(7), 601-608. https://doi.org/10.1001/jamacardio.2018.1176

Greve, G., Lab, M. J., Chen, R., Barron, D., White, P. A., Redington, A. N., & Penny, D. J. (2001). Right ventricular distension alters monophasic action potential duration during pulmonary arterial occlusion in anaesthetised lambs: evidence for arrhythmogenic right ventricular mechanoelectrical feedback. *Exp Physiol*, *86*(5), 651-657. https://doi.org/10.1113/eph8602225

Grubic, N., Hill, B., Phelan, D., Baggish, A., Dorian, P., & Johri, A. M. (2022). Bystander interventions and survival after exercise-related sudden cardiac arrest: a systematic review. *Br J Sports Med*, *56*(7), 410-416. https://doi.org/10.1136/bjsports-2021-104623

Healey, J. S., Connolly, S. J., Gold, M. R., Israel, C. W., Van Gelder, I. C., Capucci, A.,…Investigators, A. (2012). Subclinical atrial fibrillation and the risk of stroke. *N Engl J Med*, *366*(2), 120-129. https://doi.org/10.1056/NEJMoa1105575

Hoeijmakers, M. *e. a.* (2023). *pyheart-lib: A Python Library for LS-DYNA Multi-physics Heart Simulations.* Functional Imaging and Modeling of the Heart., Holzapfel, G. A., & Ogden, R. W. (2009). Constitutive modelling of passive myocardium: a structurally based framework for material characterization. *Philos Trans A Math Phys Eng Sci*, *367*(1902), 3445-3475. https://doi.org/10.1098/rsta.2009.0091

Kohl, P., Nesbitt, A. D., Cooper, P. J., & Lei, M. (2001). Sudden cardiac death by Commotio cordis: role of mechano-electric feedback. *Cardiovasc Res*, *50*(2), 280-289. https://doi.org/10.1016/s0008-6363(01)00194-8

Link, M. S. (2012). Commotio cordis: ventricular fibrillation triggered by chest impact–induced abnormalities in repolarization. *Circulation: Arrhythmia and Electrophysiology*, *5*(2), 425-432. https://doi.org/10.1161/CIRCEP.111.962712

Link, M. S., Maron, B. J., VanderBrink, B. A., Takeuchi, M., Pandian, N. G., Wang, P. J., & Estes, N. M. (2001). Impact directly over the cardiac silhouette is necessary to produce ventricular fibrillation in an experimental model of commotio cordis. *Journal of the American College of Cardiology*, *37*(2), 649-654. https://doi.org/10.1016/s0735-1097(00)01142-6

Link, M. S., Maron, B. J., Wang, P. J., VanderBrink, B. A., Zhu, W., & Estes, N. M. (2003). Upper and lower limits of vulnerability to sudden arrhythmic death with chest-wall impact (commotio cordis). *Journal of the American College of Cardiology*, *41*(1), 99-104. https://doi.org/https://doi.org/10.1016/s0735-1097(02)02669-4

Link, M. S., Wang, P. J., Pandian, N. G., Bharati, S., Udelson, J. E., Lee, M.-Y.,…Maron, B. J. (1998). An experimental model of sudden death due to low-energy chest-wall impact (commotio cordis). *New England Journal of Medicine*, *338*(25), 1805-1811.

Link, M. S., Wang, P. J., VanderBrink, B. A., Avelar, E., Pandian, N. G., Maron, B. J., & Estes, N. A. (1999). Selective activation of the K(+)(ATP) channel is a mechanism by which sudden death is produced by low-energy chest-wall impact (Commotio cordis). *Circulation*, *100*(4), 413-418. https://doi.org/10.1161/01.cir.100.4.413

Lubitz, S. A., Moser, C., Sullivan, L., Rienstra, M., Fontes, J. D., Villalon, M. L.,…Benjamin, E. J. (2013). Atrial fibrillation patterns and risks of subsequent stroke, heart failure, or death in the community. *J Am Heart Assoc*, *2*(5), e000126. https://doi.org/10.1161/JAHA.113.000126

Maron, B. J., Ahluwalia, A., Haas, T. S., Semsarian, C., Link, M. S., & Estes, N. A. (2011). Global epidemiology and demographics of commotio cordis. *Heart Rhythm*, *8*(12), 1969-1971. https://doi.org/10.1016/j.hrthm.2011.07.014

Maron, B. J., Gohman, T. E., Kyle, S. B., Estes, N. A., & Link, M. S. (2002). Clinical profile and spectrum of commotio cordis. *JAMA*, *287*(9), 1142-1146. https://doi.org/10.1001/jama.287.9.1142

Maron, B. J., Link, M. S., Wang, P. J., & Estes, N. A. (1999). Clinical profile of commotio cordis: an under appreciated cause of sudden death in the young during sports and other activities. *J Cardiovasc Electrophysiol*, *10*(1), 114-120. https://doi.org/10.1111/j.1540-8167.1999.tb00648.x

Nesbitt, A. D., Cooper, P. J., & Kohl, P. (2001). Rediscovering commotio cordis. *Lancet*, *357*(9263), 1195-1197. https://doi.org/10.1016/S0140-6736(00)04338-5

Ota, K., & Bratincsak, A. (2015). Atrial fibrillation induced by commotio cordis secondary to a blunt chest trauma in a teenage boy. *Pediatrics*, *135*(1), e199-201. https://doi.org/10.1542/peds.2014-1972

Potse, M., Dubé, B., Richer, J., Vinet, A., & Gulrajani, R. M. (2006). A comparison of monodomain and bidomain reaction-diffusion models for action potential propagation in the human heart. *IEEE Trans Biomed Eng*, *53*(12 Pt 1), 2425-2435. https://doi.org/10.1109/TBME.2006.880875

Quinn, T. A., Jin, H., Lee, P., & Kohl, P. (2017). Mechanically Induced Ectopy via Stretch-Activated Cation-Nonselective Channels Is Caused by Local Tissue Deformation and Results in Ventricular Fibrillation if Triggered on the Repolarization Wave Edge (Commotio Cordis). *Circ Arrhythm Electrophysiol*, *10*(8). https://doi.org/10.1161/CIRCEP.116.004777

Quinn, T. A., & Kohl, P. (2021). Cardiac Mechano-Electric Coupling: Acute Effects of Mechanical Stimulation on Heart Rate and Rhythm. *Physiol Rev*, *101*(1), 37-92. https://doi.org/10.1152/physrev.00036.2019

Rodero, C., Strocchi, M., Marciniak, M., Longobardi, S., Whitaker, J., O'Neill, M. D.,…Niederer, S. A. (2021). Linking statistical shape models and simulated function in the healthy adult human heart. *PLoS Comput Biol*, *17*(4), e1008851. https://doi.org/10.1371/journal.pcbi.1008851

Seo, K., Inagaki, M., Nishimura, S., Hidaka, I., Sugimachi, M., Hisada, T., & Sugiura, S. (2010). Structural heterogeneity in the ventricular wall plays a significant role in the initiation of stretch-induced arrhythmias in perfused rabbit right ventricular tissues and whole heart preparations. *Circ Res*, *106*(1), 176-184. https://doi.org/10.1161/CIRCRESAHA.109.203828

Shore, E., Moseley, G. A., DeLong, R., Register-Mihalik, J., Drezner, J. A., Dickey, G. J.,…Kucera, K. L. (2024). Incidents and patterns of *Commotio cordis* among athletes in the USA from 1982 to 2023. *Inj Prev*. https://doi.org/10.1136/ip-2024-045374

Strocchi, M., Augustin, C. M., Gsell, M. A. F., Karabelas, E., Neic, A., Gillette, K.,…Niederer, S. A. (2020). A publicly available virtual cohort of four-chamber heart meshes for cardiac electro-mechanics simulations. *PLoS One*, *15*(6), e0235145. https://doi.org/10.1371/journal.pone.0235145

ten Tusscher, K. H., Noble, D., Noble, P. J., & Panfilov, A. V. (2004). A model for human ventricular tissue. *Am J Physiol Heart Circ Physiol*, *286*(4), H1573-1589. https://doi.org/10.1152/ajpheart.00794.2003

Weisfeldt, M. L., Sitlani, C. M., Ornato, J. P., Rea, T., Aufderheide, T. P., Davis, D.,…Investigators, R. (2010). Survival after application of automatic external defibrillators before arrival of the emergency medical system: evaluation in the resuscitation outcomes consortium population of 21 million. *J Am Coll Cardiol*, *55*(16), 1713-1720. https://doi.org/10.1016/j.jacc.2009.11.077

Wijesurendra, R. S., & Casadei, B. (2019). Mechanisms of atrial fibrillation. *Heart*, *105*(24), 1860-1867. https://doi.org/10.1136/heartjnl-2018-314267

Xie, Y., Sato, D., Garfinkel, A., Qu, Z., & Weiss, J. N. (2010). So little source, so much sink: requirements for afterdepolarizations to propagate in tissue. *Biophys J*, *99*(5), 1408-1415. https://doi.org/10.1016/j.bpj.2010.06.042

Yang, S. Y., Huang, M., Wang, A. L., Ge, G., Ma, M., Zhi, H., & Wang, L. N. (2022). Atrial fibrillation burden and the risk of stroke: A systematic review and dose-response meta-analysis. *World J Clin Cases*, *10*(3), 939-953. https://doi.org/10.12998/wjcc.v10.i3.939

Zaglia, T., Pianca, N., Borile, G., Da Broi, F., Richter, C., Campione, M.,…Mongillo, M. (2015). Optogenetic determination of the myocardial requirements for extrasystoles by cell type-specific targeting of ChannelRhodopsin-2. *Proc Natl Acad Sci U S A*, *112*(32), E4495-4504. https://doi.org/10.1073/pnas.1509380112